



Design of Waste Gasification Energy Systems with Solid Oxide Fuel Cells

Rokni, Masoud

Published in:

Proceedings of the 8th International Exergy, Energy and Environmental Symposium (IEEES-9)

Publication date:

2017

Document Version

Peer reviewed version

[Link back to DTU Orbit](#)

Citation (APA):

Rokni, M. (2017). Design of Waste Gasification Energy Systems with Solid Oxide Fuel Cells. In *Proceedings of the 8th International Exergy, Energy and Environmental Symposium (IEEES-9)*

General rights

Copyright and moral rights for the publications made accessible in the public portal are retained by the authors and/or other copyright owners and it is a condition of accessing publications that users recognise and abide by the legal requirements associated with these rights.

- Users may download and print one copy of any publication from the public portal for the purpose of private study or research.
- You may not further distribute the material or use it for any profit-making activity or commercial gain
- You may freely distribute the URL identifying the publication in the public portal

If you believe that this document breaches copyright please contact us providing details, and we will remove access to the work immediately and investigate your claim.

Design of Waste Gasification Energy Systems with Solid Oxide Fuel Cells

¹Masoud Rokni

¹ Technical University of Denmark, Dept. Mechanical Engineering, Section for Thermal Energy System, Copenhagen, 2800, Denmark

* E-mail: MR@mek.dtu.dk

Abstract

Energy saving is an open point in most European countries where energy policies are oriented to reduce the use of fossil fuels, greenhouses emissions and energy independence, and to increase the use of renewable energies. In the last several years, new technologies have been developed and some of them received subsidies to increase installation and reduce cost. This article presents a new sustainable trigeneration system (power, heat and cool) based on a solid oxide fuel cell (SOFC) system integrated with an absorption chiller for special applications such as hotels, resorts, hospitals, etc. with a focus on plant design and performance. The proposal system is based on the idea of gasifying the municipal waste, producing syngas serving as fuel for the trigeneration system. Such advanced system when improved is thus self-sustainable without dependency on net grid, district heating and district cooling. Other advantage of such waste to energy system is waste management, less disposal to sanitary landfills, saving large municipal fields for other human activity and considerable less environmental impact. Although plant electrical efficiency of such system is not significant but fuel utilization factor along with free fuel, significant less pollutant emissions and self-sustainability are importance points of the proposed system. It is shown that the energy efficiency of the such small tri-geretaion system with 190 kW is more than 76%.

Keywords: SOFC, waste, gasification, absorption, energy system

I. Introduction

European countries are working to improve their energy policies of which main themes are energy saving and less pollutions. Installation of more efficient technology (such as condensing boilers, heat pumps, district cooling and district heating related to a cogeneration power plant) could help to achieve these goals. There is currently an increased interest in developing a distributed system of smaller-scale facilities at a single location, allowing electricity heat/cool to be produced and distributed close to the end user and thereby minimizing the costs associated with transportation ([Sanchez et al., 2008](#)) and ([Rokni, 2013](#)). Micro CHCP (combined heat, cool and power) for niche application falls also within this category. However, micro CHCPs face the problem of heat/cool-to power ratio that varies during the day as well as between the seasons due to the different consumption profile ([Lee and Strand, 2009](#)).

Municipal waste (MW) is one such type of biomass and is suitable for use in power plants. It presents some advantages such as the reduction of pollutants and greenhouse gas emissions and the possibility of reducing storage in landfills, as a result of which these spaces can be devoted to other human activities. Waste management is becoming a matter of crucial importance for our societies. The massive increase in the production of waste during the last decades is followed by negative consequences in the environment, whereas also there is a vital amount of raw materials that are lost due to the lack of efficient

waste treatment strategies. Hence, there is an urgent need for establishing efficient and innovative public policies concerning the handling and exploitation of waste. Traditionally waste disposal in sanitary landfills was the prevalent method related to waste management. Today this method is considered outdated due to the negative environmental impact that arise, as well as because of the high demand of large fields available for the waste disposal. A very good alternative to waste landfilling comprise the waste-to energy plants ([Niessen, 2010](#)). Currently the most mature technology is incineration, while gasification is still in the early stages of development. The remaining waste after established separation and recycling technologies in many countries (such as metals, plastics, hard papers, glass bottles and papers) would be very suitable for gasification. This is forming the basis idea of the current study.

Numerous studies have been investigated in the literature on SOFC-based hybrid systems that suggest high thermal efficiency. The majority of these studies use gas turbines as the bottoming cycle for SOFCs resulting in pressurized SOFC systems see e.g. ([Rienschke et al, 2000](#)). Steam turbines and organic rankine cycles (ORC) have also been used as a bottoming cycle, which resulted in non-pressurized SOFC stacks, see e.g. ([Rokni, 2010](#)). A few studies have been performed that utilize a Stirling engine as the bottoming cycle and the fuel cell as the topping cycle, see e.g. ([Rokni, 2013](#)).

However, studies on combined SOFC-absorption

chillers are very rare, e.g., (Weber et al., 2006) considered the potential of combined SOFC–Absorption chiller systems in Japanese office building without undergoing the detailed plant design and system operating performance. The emphasis was to indicate the market potential, CO₂ emissions and decentralized energy system, rather than the detailed analysis and performance of the units. Other studies in SOFC for residential applications as cogeneration system can be found in e.g. (Bompard et al., 2008), in which the feasibility of a 5 kW SOFC from economical view was considered. A micro CHP with SOFC for single-family detached dwellings was studied in (Farhad et al., 2010), while the impact of heat-to-power ratio for a SOFC based micro CHP for residential application in European climate was elaborated in (Liso et al. 2011). Variation of the heat to power output ratio to match the electric and hot water demands of a Japanese residence can be found in (Lamas et al., 2013).

In this article, a pioneering system is proposed which is based on a SOFC and an absorption chiller integrated with a waste gasification plant. A LiBr (Lithium Bromide) absorption chiller is chosen as a backup device to cover the cool demand while the SOFC and a heat recovery device cover the demand electricity and heat of the user. The aim of this study is not only to present a system suitable for special applications (such as hotels, resorts and hospitals) but also to design self-sustainable system that handle the produced waste to energy (power, heat and cool) after basic proven methods of recycling, which is considered as a critical problem for such particular applications.

II. System Overview

The main components of the system proposed here are a solid oxide fuel cell (SOFC) plant, an absorption chiller and a heating system (through water tank). The SOFC plant is fed by natural gas for electricity production and at the same time to use its waste heat for production of domestic heating and cooling. Figure 1 displays the integration of these components with each other.

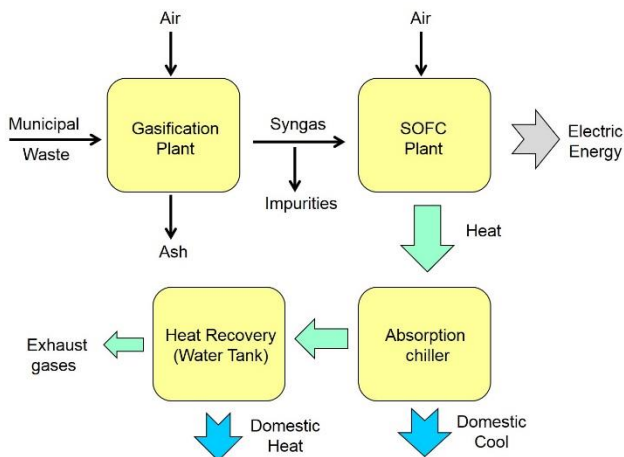


Fig. 1: General scheme of the system proposed here with the main component and energy flows.

The waste heat drives firstly the absorption chiller to produce domestic cooling. The rest of the waste energy is stored in a water tank for domestic hot water and space heating. Regulating the system allows varying cooling and heating amounts after demand. The system can be connected to the grid so that when the electricity demand exceeds the production then electricity can be drawn from the grid. In the case when the demand is lower than production, then electricity can be supplied to the grid (without considering any type of subsidy).

III. Methodology and Modelling

The thermodynamic results in this study are obtained from the Dynamic Network Analysis (DNA) simulation tool (see, e.g., Elmegaard and Houbak, 2004). This software is a result of an ongoing development process in the Thermal Energy Section of the Mechanical Department of the Technical University of Denmark. The program includes a component library, thermodynamic state models for fluids and standard numerical solvers for differential and algebraic equation systems. The component library models include heat exchangers, burners, turbo machinery, dryers, decanters, energy storages, valves and controllers, among others. The thermodynamic state models for fluids cover most of the basic fluids and such compounds as ash and tar for use in energy system analyses. DNA is a component-based simulation tool, meaning that the model is formulated by connecting components with nodes and adding operating conditions to build up a system. Next, the physical model is converted into a set of mathematical equations and solved numerically. The equations include mass and energy conservation for all components, and the nodes represent the relationships among the thermodynamic properties of the fluids in the system. The program is written in FORTRAN, and users may also contribute additional components and thermodynamic state models to the libraries. The calculation procedure is shown in Fig. 2.

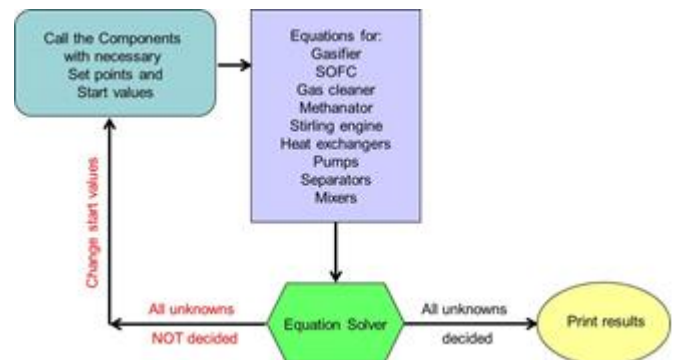


Fig. 2: Calculation procedure.

III.1. Gasifier Modeling

The gasification plant used in this study is based on the model developed in a Rokni, 2012. The model is briefly described here for clarity. A simple Gibbs reactor, where the total Gibbs free energy is minimized upon reaching chemical equilibrium, is

implemented to calculate the gas composition at a specified temperature and pressure without considering the reaction pathways (Smith et al., 2005). The Gibbs free energy of a gas (which is assumed to be a mixture of k perfect gases) is given by equation 2. Each element in the inlet gas is in balance with the outlet gas composition, implying that the flow of each constituent has to be conserved. For N elements, such balance between inlet and outlet is then expressed by means of molar fraction. The N elements correspond to H₂, O₂, N₂, CO, NO, CO₂, steam, NH₃, H₂S, SO₂, CH₄, C, NO₂, HCN (hydrogen cyanide), COS (carbonyl sulfide), Ar, and ashes (SiO₂) in the gasification process. The number of atoms of j element (H, C, O, and N) in each molecule of the entering compound i is expressed by H₂, CH₄, CO, CO₂, H₂O, O₂, N₂, and Ar. Whereas the number of atoms of element j in each molecule of the leaving compound m is expressed by H₂, O₂, N₂, CO, NO, CO₂, steam, NH₃, H₂S, SO₂, CH₄, C, NO₂, HCN, COS, Ar, and ashes. The minimization of the Gibbs free energy is mathematically formulated by introducing a Lagrange multiplier (μ) for each of the N constraints. By setting the partial derivative of this equation to zero with respect to molar outlet flow, then the corresponding function is minimized. Thus, a set of k equations are defined for each chemical compound leaving the system. Finally, it is realizable that by assuming chemical equilibrium in the gasifier, the methane content in the product gas may be underestimated. Therefore, a parameter called METHANE is applied to allow some of the methane to bypass the gasifier without undergoing any chemical reactions. The value of this parameter is assumed to be 0.01, meaning that 1% of the methane bypassed the gasifier. It may be noted that other values can be selected but due to the lack of experimental data, further investigations on the choice of this value are not conducted. Note also, such method was successfully applied by (Rokni 2014) for biomass gasification and the results agreed very well with the experimental data.

The MW composition and the properties used in this study are shown in Table 1, which is based on a previously published study (Channiwala and Parikh 2002). The only difference is that a very small amount of chlorine is also added into the composition (0.2%). It may be noted that the compositions are expressed on a dry basis (i.e., weight fraction without moisture content).

Tab. 1: Municipal waste compositions and properties used in this study

Municipal Waste Compound	Dry-based percentage
C (%)	47.6
H (%)	6
O (%)	32.9
S (%)	0.3
N (%)	1.2
Ash (%)	11.8
Cl (%)	0.2
LHV (kW), (dry basis)	19879
cp (kJ/kg)	1.71
Moisture	0.095

III.2. SOFC Modeling

The SOFC model in this study aims at representing the performance of the second-generation SOFC stacks developed by Topsoe Fuel Cell A/S (TOFC) and the Fuel Cells and Solid State Chemistry Division at Risø-DTU (Technical University of Denmark). Such SOFC type is an anode supported cell with a Ni/YSZ¹ anode, an YSZ electrolyte, and an LSM²/YSZ cathode (Christiansen et al. 2007). Anode thickness is 600 μ m, electrolyte thickness is 50 μ m and cathode thickness is 10 μ m. The SOFC stack model used in this study is the results of previous investigations such as in (Petersen et al. 2006) and (Rokni, 2014). As shown later, the model agrees very well with the experimental data at different cell operating temperatures. For sake of clarification, the model is briefly described here. The model is assumed to be zero-dimensional, enabling for application in a general computer code for calculating complicated energy systems. In such modeling, one must distinguish between electro-chemical modeling, the calculation of cell irreversibility (cell voltage efficiency) and the calculation of the species compositions at the outlet. For the electrochemical modeling, the operational voltage (E_{cell}) can be found as:

$$E_{cell} = E_{Nernst} - \Delta E_{act} - \Delta E_{ohm} - \Delta E_{conc} \quad (1)$$

where E_{Nernst} , ΔE_{act} , ΔE_{ohm} and ΔE_{conc} are the Nernst ideal reversible voltage, activation polarization, ohmic polarization and concentration polarization, respectively. Assuming that only hydrogen is electrochemically converted then the Nernst equation can be written as

$$E_{Nernst} = \frac{-\Delta g_f^0}{n_e F} + \frac{RT}{n_e F} \ln \left(\frac{p_{H_2, tot} \sqrt{p_{O_2}}}{p_{H_2O}} \right) \quad (2)$$

$$p_{H_2, tot} = p_{H_2} + p_{CO} + 4p_{CH_4} \quad (3)$$

where Δg_f^0 is the Gibbs free energy (for H₂ reaction) at standard pressure. The water-gas shift reaction is very fast; therefore, the assumption that hydrogen is the only species to be electrochemically converted is justified (see [24-25]). Because the electrochemical oxidation rate of H₂ is much higher than that of CO, then it can be assumed that hydrogen is the only species that can convert electrochemically (see e.g. Holtappels et al., 1999). In the above equations, p_{H_2} and p_{H_2O} are the partial pressures for H₂ and H₂O, respectively.

The activation polarization can be evaluated from the Butler-Volmer equation, which is isolated from other polarizations to determine the charge transfer coefficients and exchange current density from the experimental data available for different cell operating temperatures, using the curve fitting technique (see, e.g. Prentice, 1991).

¹ Yttria-stabilized zirconia.

² Lanthanum strontium manganite.

$$\begin{aligned}\Delta E_{act} &= \Delta E_{act,c} + \Delta E_{act,a} \\ &= \frac{2RT}{F} \left[\sinh^{-1} \left(\frac{i + i_n}{2i_{0,a}} \right) + \sinh^{-1} \left(\frac{i + i_n}{2i_{0,c}} \right) \right] \quad (4)\end{aligned}$$

The ohmic polarization depends on the electrical conductivity of the electrodes as well as the ionic conductivity of the electrolyte (see, e.g., Zhu and Kee, 2003). This polarization is also calibrated against experimental (for different cell operating temperatures) data for a cell with anode, electrolyte and cathode thicknesses of 600 μm , 50 μm and 10 μm , respectively.

$$\Delta E_{ohm} = \left(\frac{t_{an}}{\sigma_{an}} + \frac{t_{el}}{\sigma_{el}} + \frac{t_{ca}}{\sigma_{ca}} \right) i_d \quad (5)$$

where t_{an} , t_{el} and t_{ca} are the anode thickness, electrolyte thickness and cathode thickness, respectively. σ_{an} , σ_{el} and σ_{ca} are the conductivities of the anode, electrolyte and cathode, respectively. σ_{el} is a function of temperature, see (Rokni, 2014)

The concentration polarization is dominant at high current densities for anode-supported SOFCs, wherein insufficient amounts of reactants are transported to the electrodes and the voltage is then reduced significantly. Again, the concentration polarization is calibrated against experimental data (for different cell operating temperatures) by introducing the anode limiting current (see, e.g., Costamagna et al., 2004), in which the anode porosity and tortuosity are also included, among other parameters.

$$\Delta E_{conc} = B \left(\ln \left(1 + \frac{P_{H_2} i_d}{P_{H_2O} i_{as}} \right) - \ln \left(1 - \frac{i_d}{i_{as}} \right) \right) \quad (6)$$

where B is the diffusion coefficient and temperatures dependent. It is then calibrated using experimental data, see (Rokni, 2014).

The fuel composition at the anode outlet is calculated using the Gibbs minimization method, as described in (Smith et al. 2005). Equilibrium at the anode outlet temperature and pressure is assumed for the following species: H_2 , CO , CO_2 , H_2O , CH_4 and N_2 . Thus, the Gibbs minimization method calculates the compositions of these species at the outlet by minimizing their Gibbs energies. The equilibrium assumption is fair because the methane content in this study is very low. The methane content is mainly depended on the kinetic parameters rather than the chemical equilibrium and its reaction rate is fast (Kromp et al., 2010).

To calculate the voltage efficiency of the SOFC cells, the power production from the SOFC (P_{SOFC}) depends on the amount of chemical energy fed to the anode,

the reversible efficiency (η_{rev}), the voltage efficiency (η_v) and the fuel utilization factor (U_F). It is defined in mathematical form as

$$P_{SOFC} = \left(\begin{array}{l} LHV_{H_2} \dot{n}_{H_2,in} \\ + LHV_{CO} \dot{n}_{CO,in} \\ + LHV_{CH_4} \dot{n}_{CH_4,in} \end{array} \right) \eta_{rev} \eta_v U_F \quad (7)$$

where U_F is a set value and η_v is defined as

$$\eta_v = \frac{\Delta E_{cell}}{E_{Nernst}} \quad (8)$$

The reversible efficiency is the maximum possible efficiency, defined as the relationship between the maximum electrical energy available (change in Gibbs free energy) and the fuel's lower heating value (LHV) as follows (see, e.g., Winnick, 1997):

$$\begin{aligned}\eta_{rev} &= \frac{(\Delta \bar{g}_f)_{fuel}}{LHV_{fuel}} \quad (9) \\ (\Delta \bar{g}_f)_{fuel} &= \left[(\bar{g}_f)_{H_2O} - (\bar{g}_f)_{H_2} - \frac{1}{2} (\bar{g}_f)_{O_2} \right] y_{H_2,in} \\ &\quad + \left[(\bar{g}_f)_{CO_2} - (\bar{g}_f)_{CO} - \frac{1}{2} (\bar{g}_f)_{O_2} \right] y_{CO,in} \quad (10) \\ &\quad + \left[(\bar{g}_f)_{CO_2} + 2(\bar{g}_f)_{H_2O} - (\bar{g}_f)_{CH_4} \right] y_{CH_4,in} \\ &\quad - 2(\bar{g}_f)_{O_2}\end{aligned}$$

The partial pressures are assumed to be the average of the inlet and outlet temperatures,

$$\bar{p}_{O_2} = \left(\frac{y_{O_2,out} + y_{O_2,in}}{2} \right) \bar{p}_c \quad (11)$$

$$\bar{p}_j = \left(\frac{y_{j,out} + y_{j,in}}{2} \right) \bar{p} \quad (12)$$

$$j = \{\text{H}_2, \text{CO}, \text{CH}_4, \text{CO}_2, \text{H}_2\text{O}, \text{N}_2, \text{Ar}\}$$

A comparison between the SOFC model developed here and the experimental data is shown in Fig. 3, in terms of current density and cell voltage (IV curve). As seen from the figure, the model captures the experimental data very well at four different cell operating temperatures from 650°C to 800°C, with a standard error of less than 0.01. Different H_2 and water vapor concentrations were used when developing the model. However, only the data for 97% H_2 with 3% water vapor is shown in Fig. 3. In addition, equations for the conservation of mass (with molar flows), conservation of energy and conservation of momentum are also included in the model. The reliability of the models presented here is justified in (Rokni, 2013) with different fuels such natural gas, ethanol, and methanol. For example, the calculated plant efficiencies by the current model agrees very well with the data presented in the literature for similar plant design. Table 2 displays the main parameters for the SOFC stacks used in this study.

size plants, silicon carbide filters and/or electromagnetic filters would likely be sufficient for syngas particle purification. However, if the plant size is increased, then the fuel conditioning system may also contain cyclones and/or scrubbers prior to silicon-based filters (or electromagnetic filters). Depending on the origin/type of waste then catalytic cleaning system may also be required to decrease the sulfur and chlorine level to the acceptable levels, 1 ppm respective 10 ppm. It is also worth noting that practical engineering may be more complicated than thermodynamic analyses. It is also assumed that by separating the gasifier into two steps then it would be possible to pyrolyse and gasify the waste that is well separated from metals, glasses, hard plastics, hard papers, etc. Such waste contains mainly waste foods, organics, some plastics, some papers, etc. Note that such cleaning system may take some of the energy and alter some results but this study does not consider such effect since the detailed cleaning system is missing.

A heat exchanger called for anode preheater (AP) preheats the cleaned syngas prior to the anode side of the fuel cell. Such preheating is essential to avoid fuel cell thermal fatigue, e.g. 130°C (403 K) for about 10–15 cm long cell, which has a thickness in μm .

On the cathode side, air is first compressed and then preheated in the cathode pre-heater (CP) before entering the fuel cell. Again, such air preheating is vital to evade cell thermal tensions, e.g. 180°C (453 K) for about 10–15 cm long and 10–20 μm thick cell. The operating temperature of the fuel cell is assumed to be 780°C (1053 K), which is also used to preheat the both the incoming syngas as well as incoming air. A burner is used to burn the unused fuel out of the anode side of the fuel cell. The burner is required because all of the fuel does not react in the fuel cell stacks, owing to incomplete fuel utilization. A heat exchanger (Heat Recovery) recovers heat for both DHW (Domestic Hot Water) production and space heating. Table 4 presents system-operating parameter assumed in this study.

The absorption chiller mixes a rich refrigerant solution with a weak solution and a pump after it pumps this mixture to the generator (known as desorber). The desorber receives the waste heat and as a result, the refrigerant converts into a gaseous phase, separates the refrigerant from the liquid solution and heads the weak solution to a condenser while the rich solution goes to an absorber after passing a valve. In the condenser, the weak solution transforms into liquid by rejecting heat to a heat sink, which is either air or water but with lower inlet temperature (represented as cooling liquid in the Fig. 4). The liquid refrigerant now passes through an expansion valve where its pressure decreases (as well as its temperature) before continuing to an evaporator. In the evaporator, it absorbs heat from a higher temperature source, which in fact is the cooling demand. The refrigerant vapor then mixes with the liquid solution (coming from the other outlet of the desorber) in the absorber to form a

rich liquid solution. A pump send this mixture back to the desorber and the cycle is then closed.

Tab. 4: System operating input parameters

Parameter	Value
<i>MW mass flow (kg/h)</i>	105.3
<i>MW temperature (°C)</i>	15
<i>Drying temperature (°C)</i>	150
<i>Gasifier outlet temperature (°C)</i>	800
<i>Gasifier pressure (bar)</i>	1
<i>Gasifier pressure drop (bar)</i>	0.005
<i>Gasifier carbon conversion factor</i>	1
<i>Gasifier non-equilibrium methane</i>	0.01
<i>Steam blower isentropic efficiency</i>	0.8
<i>Steam blower mechanical efficiency</i>	0.98
<i>Air temperature into gasifier (°C)</i>	15
<i>Syngas blower isentropic efficiency</i>	0.7
<i>Syngas blower mechanical efficiency</i>	0.95
<i>Syngas cleaner pressure drop</i>	0.0049
<i>Blower air intake temperature (°C)</i>	15
<i>Blower isentropic efficiency</i>	0.7
<i>Blower mechanical efficiency</i>	0.95
<i>Gas heat exchangers pressure drop</i>	0.01
<i>Cathode preheater pressure drop (bar)</i>	0.04
<i>Anode preheater pressure drop (bar)</i>	0.01
<i>Burner inlet-outlet pressure ratio</i>	0.95

Note also that outlet temperature of the gasifier is assumed to be 800°C (1073 K) while the temperature inside the gasifier is much higher about, 1300°C (1573 K). The pressure drops assumed in the table are the results of calculating the Re-number and then friction factor in ducts. The blower (compressor) isentropic and mechanical efficiency are taken from a real one. The same is true for the steam generator. Note that the SOFC stacks are not pressurized and are working slightly above the ambient pressure. The blowers provide the pressure to overcome the pressure drops of the components along their ways (both air and fuel blowers).

V. Results and discussions

The first parameters to be studied are municipal waste moisture content and its mass flow, see Fig. 5a. These parameters may vary time to time and therefore their effect on plant performance in terms of plant power, heat and cool production shall be studied. As seen waste moisture has a positive effect on the plant efficiency, increasing moisture increases plant efficiency slightly (1.3% only). However, net power as well as cooling and heating effects decreases when moisture content is increased. Cooling, heating and net power decreases by 26.5%, 23.3% and 24.3% respectively which are significant. Variation of waste mass flow and its effect on plant power production is shown in Fig. 5b. As expected, plant cooling and heating effect as well as net power increases with waste mass flow. However, plant efficiency decreases with increasing waste mass flow. The reason is that number of stack is specified and when more fuel is fed to the stacks, then the current density increases and thereby polarization losses increases which is also dominating in this region.

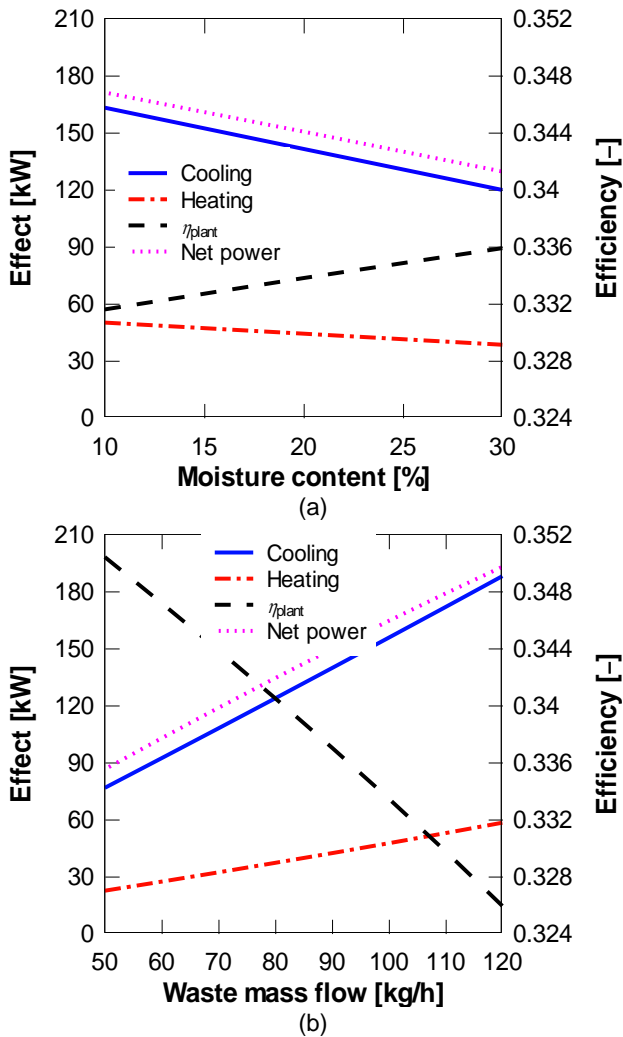


Fig. 5: Plant performance as function of waste moisture content (a) and waste mass flow (b).

Other interesting parameters to be studied are SOFC operating temperature and its utilization factor, which are shown in Fig. 6. As presented in Fig. 6a there exist an optimum SOFC operating temperature (690°C, 963K) at which plant efficiency is maxima for utilization factor of 67.5% (base case). Above this temperature plant efficiency decreases and thereby fuel cell net power decreases as well. This in turn leaves more heat to be available for heating and cooling devices and therefore their production will increase as a result. Similarly, below this optimum temperature plant efficiency as well as fuel cell net power decreases leaving more heat for the heating and cooling devices and thereby their effect increases.

Fig. 6b displays SOFC utilization factor versus plant efficiency and produced trigeneration effect. It is also shown that for utilization factor of 70%, plant efficiency and plant net power becomes maximum (optimum point). However, with increasing utilization factor, the plant heating effect increases while the plant cooling effect decreases until a certain point at which suddenly cell voltage decreases significantly because of cell polarization losses (after about 77%). Due to sudden decrease in fuel cell power, heat available for heating and cooling devices increases and thereby produced heating and cooling effects

increases suddenly as the consequence.

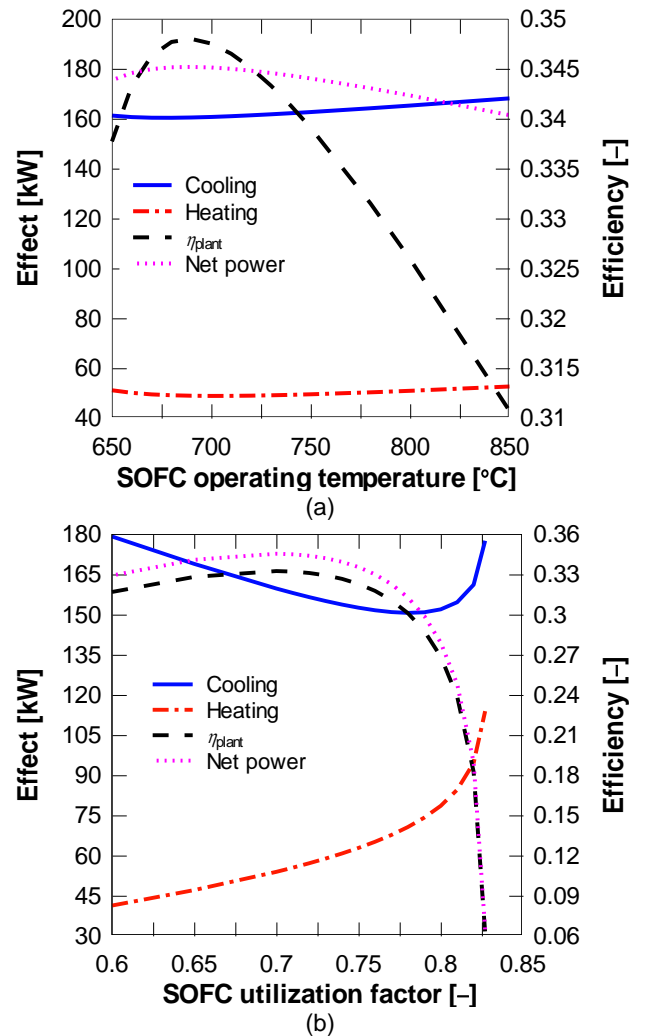


Fig. 6: Plant performance as function of SOFC operating temperature (a) and SOFC utilization factor (b).

It is worth to mention that the obtained results are valid when other parameters remains unchanged such as number of stack (160), fuel mass flow (105 kg/h) and either SOFC operating temperature or its utilization factor. Changing these parameters from the base case alters the obtained results here, and other values may be attained. For example, the optimum SOFC operating temperature will change when fuel mass flow and number of stack changes.

V.1. Effect of Desorber Outlet Temperature

Another parameter to be investigated is the desorber outlet temperature which is assumed to be 135°C (408 K) in the base case. However, this value is rather high for such plant since off-gases are rather clean after the cleaning system and therefore surface oxidation shall be neglected and the attention can be paid on the dewpoint only (avoiding condensation). The dewpoint of such gases is assumed approximately 70°C (353 K), when leaving the heat exchanger for heat production. Thus, the temperature out of the desorber shall be slightly higher.

Decreasing the desorber outlet temperature would be in favor of cooling effect as presented in Fig. 7, while it

has a negative impact on heat production. For example, decreasing desorber outlet temperature from 135°C (408K) to 90°C (363 K) increases cooling effect by 11.5% while heat production decreases by 66.8%. Note that the plant net power as well as its thermal efficiency does not change when varying desorber outlet temperature. In practical design, the plant functionality in terms of heating and cooling effect can be controlled via the mass flow of the the off gases passing through the desorber (or a temperature sensor). The figure also displays that plant fuel utilization (ϵ , total efficiency) increases slightly, from about 0.71 to about 0.76 when desorber temperature changes from 80°C to 160°C.

It shall be noted that the mass flow of the water (other side of the heat recovery heat exchanger) is assumed to be 0.1 kg/s, although any other values could be assumed since its value does not alter the results obtained here.

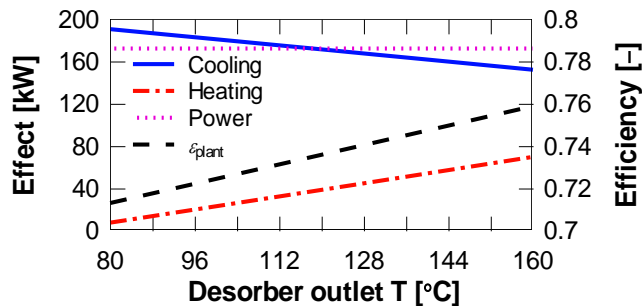


Fig. 7: Plant performance as function of desorber outlet temperature.

V.2. Effect of Weak Solution and Rich Solution

The weak and rich solutions in the base case were assumed to be 0.548 and 0.593 respectively. Choosing other values than these values effect on the cool production as evaluated in Fig. 8.

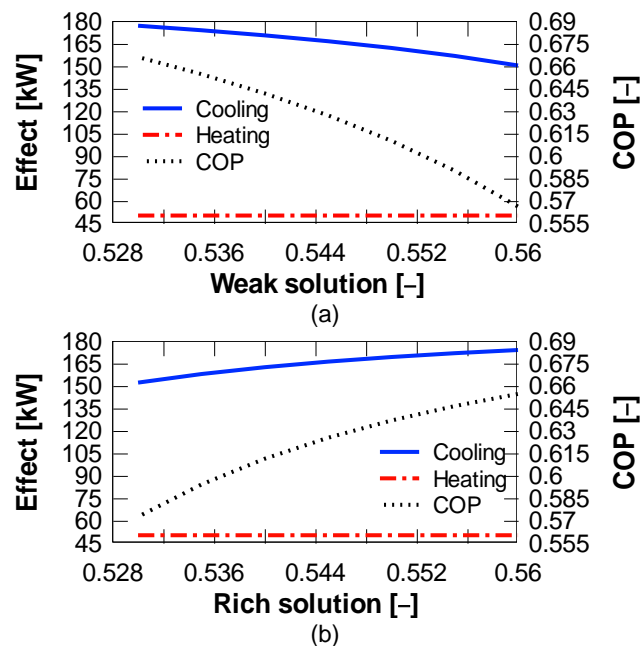


Fig. 8: Effect of weak and rich solution on cooling and heating effect.

The figure shows that decreasing the weak solution as well as increasing the rich solution increases the cooling effect. As mentioned above, the COP of the absorptions chillers are rather small and usually lie between 0.5 and 1.5, which is also justified in Fig. 8. COP increases by decreasing weak solution and increasing rich solution and the average is about 0.6 in this study. It is obvious that the COP can be increased if the difference between the rich and weak solutions increases. To reach a value of 1 the difference must be about 0.6 (compared to 0.048 in the base case studied here). Such increased difference demands technical refinement and component improvement, which is out of the scope of this study.

VI. Conclusions

A trigeneration system based on municipal waste, solid oxide fuel cell and absorption chiller is presented and thermodynamically analyzed. Detailed balance of plant is designed and considered. It has been shown that plant electrical efficiency increases by fuel moisture content with specified waste mass flow and number of fuel cell stacks.

It is also revealed that for the specified waste composition and number of cells, the optimum SOFC utilization factor is 70% and plant electric efficiency decreases significantly if utilization is beyond about 77% (mainly due to increase in concentration losses).

Fuel utilization (energy efficiency) beyond 0.76 is easily achievable by such trigeneration system when heating effect, cooling effect and power are included for a system, with about 190 kW electricity production.

Producing more heat results in improved plant energy efficiency (total efficiency) in expense of less cooling effect. Other conclusions among others are that increasing waste mass flow is in favour of electricity, heat and cool production, while increasing waste moisture content decreases them.

Nomenclature

E	: Electricity, V
F	: Faradays constant, 96487 C.mol ⁻¹
g^0	: standard Gibbs free energy, J.mol ⁻¹
g_f	: Gibbs free energy, J.mol ⁻¹
i	: current density, mA.cm ⁻²
\dot{m}	: mass flow, kg/s
\dot{n}	: molar reaction rate, mol.s ⁻¹
n_e	: number of electron
P	: power, W
P	: pressure, bar
R	: universal gas constant, 8314, J.kmol ⁻¹ .K ⁻¹
T	: temperature, K
U_F	: fuel utilization factor

Greek Letters

Δ	: difference, –
η	: efficiency, –
ρ	: density, kg/m ³
h	: enthalpy, kJ/kg

Subscripts

act : activation
 ohm : ohmic
 conc : concentration
 inv : inventor
 rev : reversible
 v : voltage

Abbreviations

AP : Anode Preheater
 CP : Cathode Preheater
 COP : Coefficient of Performance
 GAP : Gasifier Air Preheater
 LHV : Lower Heating Value
 MW : Municipal Waste
 SG : Steam generator
 SOFC : Solid Oxide Fuel Cell

References

- Bompard E., Napoli R., Wan B. and Orsello G. 2008. Economics evaluation of a 5kW SOFC power system for residential use. *Hydrogen Energy* 33:3243–47.
- Channiwala S.A. and Parikh P.P. 2002. A unified correlation for estimating HHV of solid, liquid and gaseous fuels. *Fuel* 81(8):1051-63.
- Christiansen N., Hansen J.B., Holm-Larsen H., Linderoth S., Larsen P.H., Hendriksen P.V. and Hagen A. 2007. Solid oxide fuel cell development at Topsoe fuel cell and Risø. *J Electrochemical Society* 7(1):31–38.
- Costamagna P., Selimovic A., Del Borghi M. and Agnew G. 2004. Electrochemical model of the integrated planar solid oxide fuel cell (IP-SOFC), *Chemical Engineering* 102(1):61–69.
- Elmegaard B., Houbak N. 2005. DNA - A general energy system simulation tool. *Proceeding of SIMS 2005*, Trondheim, Norway.
- Farhad S., Hamdullahpur F. and Yoo Y. 2010. Performance evaluation of different configurations of biogas-fuelled SOFC micro-CHP systems for residential applications. *Hydrogen Energy* 35:3758–68.
- Holtappels P., DeHaart L.G.J., Stimming U., Vinke I.C. and Mogensen M. 1999. Reaction of CO/CO₂ gas mixtures on Ni-YSZ cermet electrode. *Applied Electrochemistry* 29:561–568.
- Kromp A., Leonide A., Timmermann H., Weber A. and Ivers-Tiffée E. 2010. Internal Reforming Kinetics in SOFC-Anodes. *ECS Transactions* 28(11):205–215.
- Lamas J., Shimizu H., Matsumura E. and Senda J. 2013. Fuel consumption analysis of a residential cogeneration system using a solid oxide fuel cell with regulation of heat to power ratio. *Hydrogen Energy* 38:16338–43.
- Lee K.H. and Strand R.K.. 2009. SOFC cogeneration system for building applications, part 2: System configuration and operating condition design. *Renewable Energy* 34(12):2839–46.
- Liso V., Brandon N., Zhao Y., Nielsen M.P. and Koer S.K. 2011. Analysis of the impact of heat-to-power ratio for a SOFC-based mCHP system for residential application under different climate regions in Europe. *Hydrogen Energy* 36:13715–26.
- Morris M. and Waldheim L. 1998. Energy recovery from solid waste fuels using advanced gasification technology. *Waste Management* 18(6-8):557-564.
- Niessen W.R., 2010. *Combustion and Incineration Processes: Applications in Environmental Engineering*, fourth ed. CRC Press, Massachusetts, USA.
- Petersen T.F., Houbak N. and Elmegaard B. 2006. A zero-dimensional model of a 2nd generation planar SOFC with calibrated parameters. *Int J Thermodyn* 9(4):161-9.
- Riensch E., Achenbach E., Froning D., Haines M.R., Heidug W.K., Lokurlu A. and Adrian S. 2000. Clean combined-cycle SOFC power plant–cell modeling and process analysis. *Power Sources* 86(1–2):404–10.
- Rokni M. 2010. Plant characteristics of an integrated solid oxide fuel cell cycle and a steam cycle. *Energy* 35:4691–99.
- Rokni M. 2012. Thermodynamic Analysis of an Integrated Gasification Plant with Solid Oxide Fuel Cell and Steam Cycle. *J. Green* 2(2-3):71–86.
- Rokni M. 2013. Thermodynamic analysis of SOFC (solid oxide fuel cell) – Stirling hybrid plants using alternative fuels. *Energy* 61:87–97.
- Rokni M. 2014. Biomass Gasification Integrated with a Solid Oxide Fuel Cell and Stirling Engine. *Energy* 77:6–18.
- Sanchez D., Chacartegui R., Torres M. and Sanchez T. 2008. Stirling based fuel cell hybrid systems: an alternative for molten carbonate fuel cells. *Power Sources* 192:84–93.
- Smith J.M., Van Ness H.C. and Abbott M.M. 2005. *Introduction to chemical engineering thermodynamics*. 7th edition, Boston: McGraw-Hill.
- Weber C., Koyama M. and Kraines S. 2006. CO₂-emissions reduction potential and costs of a decentralized energy system for providing electricity, cooling and heating in an office-building in Tokyo. *Energy* 31:3041–3061.
- Winnick J. 1997. *Chemical engineering thermodynamics*, John Wiley & Sons, New Yourk.
- Zhu H. and Kee R.J. 2003. A general mathematical model for analyzing the performance of fuel-cell membrane-electrode assemblies. *Power Sources* 117:61–74.